

Zero-temperature equation of state of quasi-one dimensional H₂

M.C. Gordillo, J. Boronat and J. Casulleras

Departament de Física i Enginyeria Nuclear, Campus Nord B4-B5, Universitat Politècnica de Catalunya. E-08034 Barcelona, Spain

(April 26, 2024)

We have studied molecular hydrogen in a pure 1D geometry and inside a narrow carbon nanotube by means of the diffusion Monte Carlo method. The one-dimensionality of H₂ in the nanotube is well maintained in a large density range, this system being closer to an ideal 1D fluid than liquid ⁴He in the same setup. H₂ shares with ⁴He the existence of a stable liquid phase and a quasi-continuous liquid-solid transition at very high linear densities.

PACS numbers:67.70.+n,02.70.Lq

The experimental finding in 1991 [1] of carbon nanotubes opened brand new possibilities both in technology and in fundamental physics. The nanoscale of these new materials has led to the discovery of novel mechanical, chemical and electrical properties [2] that suggest exciting new technological applications. One of the more relevant features of these new materials is their large adsorption capability compared with that of a graphite planar substrate. In fact, the enhanced Van der Waals interaction when particles are adsorbed inside a single nanotube, or in the interstitial sites of single wall carbon nanotube (SWCN) bundles, may allow the density of the adsorbed substrate to be high enough for the bundles to serve as gas storage devices. Special interest exists in the physisorption of hydrogen [3–7] in the quest for a fuel cell efficient enough to be used as a pollution-free energy carrier. It has been recently suggested that SWCN with diameters of the order of a nanometer can be the best candidates to approach the pursued level of packing [3].

From a more fundamental point of view, the strong confinement of particles adsorbed in the carbon channels of a SWCN bundle, with diameters ranging from 7 to 40 Å and an width to length ratio of ~ 1000 , offers the possibility of an experimental realization of a quasi-one dimensional system. Moreover, if the temperature is low enough one is dealing with a unique opportunity of studying a nearly one-dimensional quantum fluid. In a recent experiment, Teizel *et al.* [8] have unambiguously observed the quasi-one dimensional behavior of ⁴He adsorbed in a SWCN bundle by measuring its desorption rate. On the other hand, theoretical studies in the limit of zero temperature and strictly one dimension have proved the existence of a liquid state with a binding energy in the milli-Kelvin scale [9–11]. Using the diffusion Monte Carlo (DMC) method, we also compared the ideal 1D geometry system with a realistic situation in which ⁴He is adsorbed in a narrow nanotube [10]. The aim of the present work is to extend the theoretical study to the appealing case of H₂ that, besides its technological relevance, might offer the existence of a homogeneous liquid phase at zero temperature. It is worth noticing that both

bulk and two-dimensional H₂, are solid in this temperature limit. Liquid phases have only been observed in theoretical calculations of small clusters [12] and in 2D geometries with localized alkaline impurities [13].

We have studied molecular hydrogen at zero temperature in a one-dimensional (1D) array and inside a single walled carbon nanotube (T) of radius $R = 3.42$ Å, which corresponds to a (5,5) armchair tube [14]. The technique used is the DMC method, which has become in the last decades one of the most efficient theoretical tools, from the microscopic point of view, to deal with quantum fluids. The DMC method solves the N -body imaginary-time Schrödinger equation

$$-\frac{\partial f(\mathbf{R}, t)}{\partial t} = -D\nabla_R^2 f(\mathbf{R}, t) + D\nabla_R \cdot (\mathbf{F} f(\mathbf{R}, t)) + (E_L(\mathbf{R}) - E)f(\mathbf{R}, t) \quad (1)$$

in which $f(\mathbf{R}, t) = \psi(\mathbf{R})\Psi(\mathbf{R}, t)$, $D = \hbar^2/2m$, $E_L(\mathbf{R}) = \psi(\mathbf{R})^{-1}H\psi(\mathbf{R})$ is the local energy, and $\mathbf{F}(\mathbf{R}) = 2\psi(\mathbf{R})^{-1}\nabla\psi(\mathbf{R})$ is the so-called drift force. The time-independent wave function $\psi(\mathbf{R})$ acts as an important sampling function and is chosen as a trial model usually adjusted at a variational Monte Carlo (VMC) level. In bosonic systems like the present one the DMC method provides exact results apart from statistical uncertainties. More specific details of DMC may be drawn from Refs. [15,16].

A relevant issue in a microscopic study is the nature of the interspecies interaction. We have considered the H₂ molecules interacting via the isotropic semiempirical potential from Silvera and Goldman (SG) [17] that has been extensively used in path integral Monte Carlo (PIMC) and DMC calculations of bulk [18], clusters [12] and H₂ films [19]. The SG is a pair potential that incorporates to some extent the effect of three-body interactions by means of an effective two-body term of the form C_9/r^9 . On the other hand, the isotropy of the potential is well justified if one considers that at very low temperatures almost all the H₂ molecules are para-hydrogen species, i.e., they are in the J=0 rotational state. In the simulations of H₂ inside a nanotube, we consider a cylindrically sym-

metric potential as suggested by Stan and Cole [20]. In that simplified model, the interactions between C atoms and H₂ molecules are axially averaged out resulting in a potential which only depends on the distance to the center of the tube. It has been proved [5] that the differences between that smoothed potential and a potential which is built up as an explicit sum of individual C-H₂ interactions are not significant and surely smaller than the relative uncertainty in the (σ, ϵ) Lennard-Jones parameters. Considering $\sigma = 2.97$ Å and $\epsilon = 42.8$ K, the symmetric potential felt by a H₂ molecule in a (5,5) tube has a depth of 42ϵ , three times larger than the attraction of the same molecule in a flat graphitic surface.

The use of importance sampling in DMC requires the introduction of a trial wave function that guides the diffusion process to relevant regions of the walkers phase space. In the 1D system, we consider

$$\Psi^{1D}(\mathbf{R}) = \Psi_J(\mathbf{R}), \quad (2)$$

with $\Psi_J(\mathbf{R}) = \prod_{i < j} \exp \left[-\frac{1}{2} \left(\frac{b}{r_{ij}} \right)^5 \right]$ a Jastrow wave function with a McMillan two-body correlation factor. Inside the nanotube, H₂ molecules interact with the walls of the cylinder and therefore we have added an additional one-body term

$$\Psi^T(\mathbf{R}) = \Psi_J(\mathbf{R}) \Psi_c(\mathbf{R}) \quad (3)$$

with $\Psi_c(\mathbf{R}) = \prod_i^N \exp(-c r_i^2)$, r_i being the radial distance of the particle to the center, to avoid the hard core of the H₂-nanotube interaction.

Theoretical calculations of 1D ⁴He agree in predicting a liquid-solid phase transition at high linear densities [9–11]. This transition which is only possible at absolute zero temperature looks like a nearly continuous one without a measurable difference between the melting and freezing densities. Following the same procedure that in our previous work in helium, we have explored the existence of such a transition in H₂. In this ordered phase, we modify the trial wave function in both the 1D system and inside the nanotube by multiplying them by a z -localized factor $\Psi_s(\mathbf{R}) = \prod_i^N \exp(-a(z_i - z_{is})^2)$. The sites z_{is} are equally-spaced points in both the 1D line and the axial direction of the nanotube.

The variational parameters a , b and c have been optimized by means of VMC calculations. In the liquid phase and near the equilibrium density $b = 3.759$ Å, with a slight increase with density (at $\lambda = 0.277$ Å⁻¹, $b = 3.789$ Å), whereas $c = 4.908$ Å⁻² is kept fixed for all λ values. In the solid phase, $b = 3.404$ Å, $a = 0.799$ Å⁻² and $c = 5.136$ Å⁻², with a negligible λ dependence in the region analyzed.

The possible existence of a liquid-solid phase transition at high linear density has been studied in both 1D and inside a narrow nanotube. In Table I, results for the energy per particle of both systems are reported for

the liquid ($a = 0$) and solid ($a \neq 0$) phases. The comparison between the energies of both phases at the same density shows that their difference changes sign in going from $\lambda = 0.312$ Å⁻¹ to $\lambda = 0.304$ Å⁻¹ in 1D and from $\lambda = 0.320$ Å⁻¹ to $\lambda = 0.312$ Å⁻¹ in the tube. Above these densities, the system prefers to be localized in a solid-like structure with a difference $|E(s) - E(l)|$ that increases with λ . When the density decreases the liquid phase is energetically preferred and again the size of the difference $|E(s) - E(l)|$ increases when λ diminishes. The density value at which this difference becomes zero is estimated to be $\lambda = 0.309$ Å⁻¹ in 1D and $\lambda = 0.315$ Å⁻¹ in the tube, being not possible to distinguish between freezing and melting densities. As previously studied in ⁴He [10] it appears to be a nearly continuous phase transition located at a density close to the inverse of the location of the minimum of the respective pair potential ($r_m^{-1} = 0.337$ Å⁻¹ vs $\lambda_s = 0.358$ Å⁻¹ for helium, and $r_m^{-1} = 0.291$ Å⁻¹ vs $\lambda_s = 0.309, 0.315$ Å⁻¹ for molecular hydrogen).

Inside the nanotube (T), the energies are much more negative than in 1D due to the strong attraction of the carbon substrate: the binding energy of a single H₂ molecule in the tube is $E_b = -1539.87 \pm 0.11$ K. Looking at the T-energy results contained in Table I one realizes that also in this case a transition occurs at a density very close to the 1D one. It is remarkable that both in 1D and T, H₂ remains liquid below the liquid-solid transition density, and thus a homogeneous liquid phase at zero pressure is predicted. That result contrasts with the theoretically and experimentally well established solid phase in 3D [21] and the 2D solid phase predicted by a PIMC calculation [19].

The equations of state of liquid H₂ near the equilibrium density for both the 1D and T systems are shown in Fig. 1. In order to make the energy scales compatible we have subtracted the single binding energy E_b to the T results. The lines in the figure correspond to the third-degree polynomial fits in the form

$$\frac{E}{N} = e_0 + A \left(\frac{\lambda - \lambda_0}{\lambda_0} \right)^2 + B \left(\frac{\lambda - \lambda_0}{\lambda_0} \right)^3. \quad (4)$$

The best set of parameters e_0 , λ_0 , A and B are reported in Table II. The equilibrium densities in both systems are the same considering their respective uncertainties but the binding energy $e_0 = e(\lambda_0)$ is larger when H₂ is inside the nanotube. The difference between the 3D geometry (T) and the idealized one (1D) can be quantified by means of the adimensional parameter

$$\Delta^T = \frac{(E^T - E_b^T) - E_{1D}}{(E^T - E_b^T)} \quad (5)$$

In the present system, around λ_0 , $\Delta^T = 3.5$ % which emphasizes the proximity between the real system and the idealized one. It is worth noting that in ⁴He inside the same nanotube we obtained $\Delta^T = 90$ % [10], and

therefore H_2 seems a better candidate to experimentally achieve a 1D condensed phase. That significant difference between helium and hydrogen may be understood taking into account that the difference between the hard-core size of the C-He interaction ($\sigma_{\text{C-He}} = 2.74 \text{ \AA}$) and the C- H_2 one ($\sigma_{\text{C-H}_2} = 2.97 \text{ \AA}$) is magnified in a (5,5) tube because its small radius ($R = 3.42 \text{ \AA}$).

In Fig. 2, the density dependence of the pressure for both the 1D and T systems is reported from equilibrium up to the liquid-solid transition density. As a matter of comparison, the same results for ^4He are also plotted. Both in H_2 and ^4He the pressure increases faster in the 1D geometry (P_λ) than in the tube (P) due the transverse degree of freedom that particles have in the latter case (notice the proportionality between the scales of P and P_λ in Fig. 2, $P_\lambda/P = \pi R^2$). At a given density λ , the difference between the T and 1D pressures is smaller in H_2 than in ^4He . For example, at the respective transition densities that difference is more than one and a half times larger in helium than in hydrogen. Therefore, the one-dimensionality of H_2 inside the nanotube is well maintained in all the liquid regime in contrast with ^4He , in which the departure from such an idealized model already appears around the equilibrium density and increases significantly with λ . Also apparent from Fig. 2 is a much smaller compressibility in H_2 than in ^4He . In the 1D geometry at $\lambda = \lambda_0$ the velocity of sound in H_2 is $c = 736.1 \pm 0.2 \text{ m/sec}$ to be compared with $c = 7.98 \pm 0.07 \text{ m/sec}$ in ^4He at $\lambda = \lambda_0(^4\text{He}) = 0.062 \text{ \AA}^{-1}$. The velocity of sound drops to zero at the spinodal point that, according to the equation of state (Table II), is located at densities $0.210 \pm 0.001 \text{ \AA}^{-1}$ and $0.209 \pm 0.001 \text{ \AA}^{-1}$ for the 1D and T systems, respectively.

The spatial structure of molecular hydrogen in the 1D array and inside the nanotube has also been analyzed by means of the two-body radial distribution function, $g(z)$, and its Fourier transform, the static structure factor $S(k)$. In Fig. 3, 1D results for $g(z)$ are reported at both the equilibrium density for the liquid phase, and in the solid-liquid transition region ($\lambda = 0.312 \text{ \AA}^{-1}$). The corresponding results for H_2 inside the nanotube are indistinguishable from the 1D results in the scale shown in Fig. 3. The solid $g(z)$ shows a strongly localized order around the equally spaced z -sites that decreases very slowly when z increases. The result for $g(z)$ at $\lambda = \lambda_0$ manifests the nature of a dense fluid with an appreciable structure that decreases slowly and shows residual ordering up to large z distances. A comparison with previous DMC results on helium at the same density shows that the height of the ^4He peaks is approximately an 80 % of the corresponding ones in H_2 , but with a z -ordering that also survives up to large distances; the additional 20 % comes from the sizeable difference between the well depths of the respective interaction potentials.

The significant differences in structure between the low and high density regimes are reflected even more clearly

in the static structure factors. In Fig. 4, results for $S(k)$ corresponding to the same densities reported in Fig. 3 are shown. At high density, a characteristic result for a solid phase is obtained with a regular k -spacing according to the only periodicity allowed by the 1D geometry. At $\lambda = \lambda_0$, $S(k)$ shows a first peak reflecting the localization observed in $g(z)$ (Fig. 3), and a subsequent very smoothed maximum as expected in a homogeneous liquid phase.

In conclusion, we have studied the zero-temperature equation of state of molecular hydrogen in a 1D geometry and inside a narrow nanotube by means of the diffusion Monte Carlo method. The 1D calculation predicts the existence of a self-bound system with a binding energy of -4.8 K and a quasi-continuous liquid-solid transition at high density. The comparison with a real system, hydrogen in a nanotube, points to a close proximity between its properties and the ones of the 1D limit. The prediction of a liquid H_2 phase inside a (5,5) carbon nanotube is one of the main conclusions of the present work. The high one-dimensionality of this system would preclude a superfluid behavior but the use of wider nanotubes can provide a proper setup to observe the so-long desired superfluidity in molecular hydrogen. We expect the present work could encourage experimentalists to explore such a intriguing possibility.

This research has been partially supported by DGES (Spain) Grants N^o PB96-0170-C03-02 and PB98-0922, and DGR (Catalunya) Grant N^o 1999SGR-00146. M. C. G. thanks the Spanish Ministry of Education and Culture (MEC) for a postgraduate contract. We also acknowledge the supercomputer facilities provided by the CEPBA.

-
- [1] S. Ijima, *Nature* **354**, 56 (1991).
 - [2] P. M. Ajayan and T. W. Ebbesen, *Rep. Prog. Phys.* **60**, 1025 (1997).
 - [3] A. C. Dillon, K. M. Jones, T. A. Bekkedahl, C. H. Kiang, D. S. Bethune, and M. J. Heben, *Nature* **386**, 377 (1997).
 - [4] F. Darkrim and D. Levesque, *J. Chem. Phys.* **109**, 4981 (1998).
 - [5] G. Stan and M. W. Cole, *J. Low Temp. Phys.* **110**, 539 (1998).
 - [6] M. Rzepka, P. Lamp, M. A. de la Casa-Lillo, *J. Phys. Chem. B* **102**, 10894 (1998).
 - [7] Q. Wang and J. K. Johnson, *J. Chem. Phys.* **110**, 577 (1999).
 - [8] W. Teizer, R. B. Hallock, E. Dujardin, and T. W. Ebbesen, *Phys. Rev. Lett.* **82**, 5305 (1999); *Phys. Rev. Lett.* **84**, 1844 (2000).
 - [9] E. Krotscheck and D. Miller, *Phys. Rev. B* **60**, 13038 (1999).
 - [10] M. C. Gordillo, J. Boronat, and J. Casulleras, *Phys. Rev. B* **61**, R878 (2000).

- [11] M. Boninsegni and S. Moroni, J. Low Temp. Phys. **118**, 1 (2000).
- [12] P. Sindzingre, D. M. Ceperley, and M. L. Klein, Phys. Rev. Lett. **67**, 1871 (1991).
- [13] M. C. Gordillo and D. M. Ceperley, Phys. Rev. Lett. **79**, 3010 (1997).
- [14] N. Hamada, S. Sawada, and A. Oshiyama, Phys. Rev. Lett. **68**, 1579 (1992).
- [15] J. Boronat and J. Casulleras, Phys. Rev. B **49**, 8920 (1994).
- [16] B. L. Hammond, W. A. Lester Jr., and P. J. Reynolds, *Monte Carlo Methods in Ab Initio Quantum Chemistry* (World Scientific, Singapore, 1994).
- [17] I. F. Silvera and V. V. Goldman, J. Chem. Phys. **69**, 4209 (1978).
- [18] E. Cheng and K. B. Whaley, J. Chem. Phys. **104**, 3155 (1996).
- [19] M. Wagner and D. M. Ceperley, J. Low Temp. Phys. **94**, 161 (1994).
- [20] G. Stan and M. W. Cole, Surf. Sci. **395**, 280 (1998).
- [21] I. F. Silvera, Rev. Mod. Phys. **52**, 393 (1980).

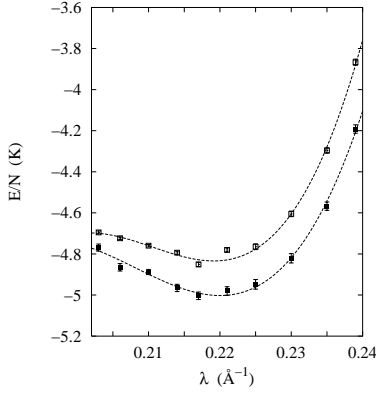


FIG. 1. Energy per particle of H_2 as a function of the linear density. Open squares are the 1D results, and filled squares are the T energies having subtracted the binding energy of a single molecule E_b . The lines are the result of the polynomial fit (Eq. 4) with the optimal parameters reported in Table II.

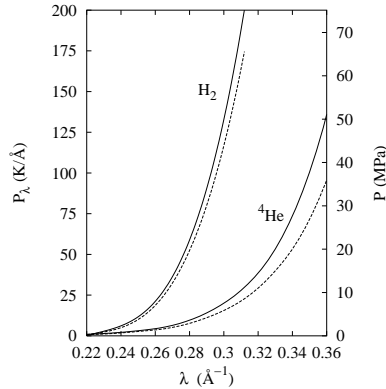


FIG. 2. 1D (P_λ , solid line) and T (P , dashed line) pressures for H_2 and ^4He as a function of the linear density.

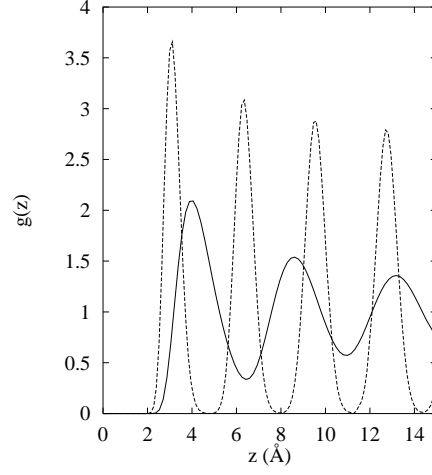


FIG. 3. Two-body radial distribution function for 1D H_2 at equilibrium (solid line) and at the liquid-solid transition density (dashed line).

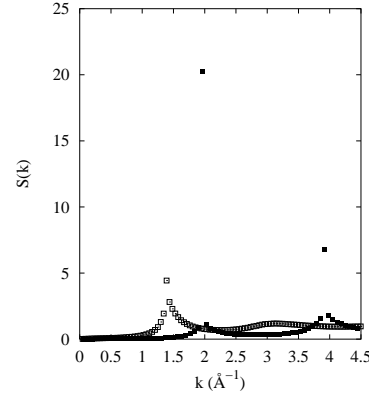


FIG. 4. Static structure function for 1D H_2 near equilibrium (open symbols) and at the liquid-solid transition density (filled symbols).

λ (\AA^{-1})	E/N (1D, $a = 0$)	E/N (1D, $a \neq 0$)	E/N (T, $a = 0$)	E/N (T, $a \neq 0$)
0.329	98.083 ± 0.034	97.963 ± 0.016	-1453.99 ± 0.06	-1454.69 ± 0.04
0.320	72.567 ± 0.013	72.523 ± 0.007	-1476.74 ± 0.05	-1476.88 ± 0.01
0.312	53.264 ± 0.010	53.227 ± 0.010	-1493.790 ± 0.019	-1493.720 ± 0.002
0.304	38.581 ± 0.018	38.636 ± 0.014	-1506.570 ± 0.03	-1506.540 ± 0.011
0.290	19.203 ± 0.010	19.260 ± 0.003	-1523.730 ± 0.017	-1523.600 ± 0.02

TABLE I. Energies per particle in K at high linear densities λ for 1D and T H_2 systems. $a = 0$ and $a \neq 0$ correspond to the liquid and solid phases, respectively.

Parameter	1D H_2	H_2 in a tube
λ_0 (\AA^{-1})	0.2191 ± 0.0004	0.2200 ± 0.0006
e_0 (K)	-4.834 ± 0.007	-1544.880 ± 0.016
A (K)	65.7 ± 3.6	69.7 ± 4.9
B (K)	556.0 ± 46.6	429.7 ± 73.9
χ^2/ν	1.98	1.5

TABLE II. Parameters of the equation of state (Eq. 4) for the two systems studied.